Plant-Limited Co-Design of an Energy-Efficient Counterbalanced Robotic Manipulator

James T. Allison[1]
Assistant Professor
Mem. ASME
University of Illinois at Urbana-Champaign,
Urbana, IL 61801
e-mail: jtalliso@illinois.edu

Modifying the design of an existing system to meet the needs of a new task is a common activity in mechatronic system development. Often, engineers seek to meet requirements for the new task via control design changes alone, but in many cases new requirements are impossible to meet using control design only; physical system design modifications must be considered. Plant-limited co-design (PLCD) is a design methodology for meeting new requirements at minimum cost through limited physical system (plant) design changes in concert with control system redesign. The most influential plant changes are identified to narrow the set of candidate plant changes. PLCD provides quantitative evidence to support strategic plant design modification decisions, including tradeoff analyses of redesign cost and requirement violation. In this article the design of a counterbalanced robotic manipulator is used to illustrate successful PLCD application. A baseline system design is obtained that exploits synergy between manipulator passive dynamics and control to minimize energy consumption for a specific pick-and-place task. The baseline design cannot meet requirements for a second pick-and-place task through control design changes alone. A limited set of plant design changes is identified using sensitivity analysis, and the PLCD result meets the new requirements at a cost significantly less than complete system redesign. [DOI: 10.1115/1.4024978]

1 Introduction

Mechatronic systems exhibit tight coupling between physical system (plant) design and control system design, requiring an integrated approach for developing high-performance systems [1,2]. In conventional sequential mechatronic design, the physical system is designed completely before control system design [1,3,4]; this approach fails to produce system-optimal results [5]. Physical system design should be informed by control system considerations. More integrated design methods are required as the complexity and scale of mechatronic design problems increase.

One approach that accounts fully for plant and control system interactions is co-design, an optimization-based design methodology where physical system and control system design are considered simultaneously (see work by Li et al. [3], Fathy et al. and Fathy [5,6], Peters et al. [7], and Reyer et al. [8] for examples of co-design studies). Using this approach, we can capitalize on the synergy between physical and control system design decisions to produce systems with superior performance. Fully concurrent co-design, however, can be a challenge to implement. It is computationally intensive, often new system models must be developed, and its tightly integrated nature may not mesh well with the compartmentalized organizational structures present in many engineering firms. Peters et al. introduced an intermediate approach that produces better results than conventional sequential design, yet exhibits lower computational expense than co-design employs. This approach employs control proxy functions to augment the plant design problem and account for control design needs during plant optimization [9]. While the result of this modified sequential approach is not system optimal except in special cases, the augmented plant design problem is more closely aligned with the overall system design objective.

Repurposing existing mechatronic systems to meet the needs of new applications presents another opportunity to incorporate integrated design approaches into engineering practice. Engineers are often asked to modify existing mechatronic systems to meet the requirements of a new task instead of developing new systems from scratch. This reduces redevelopment and manufacturing costs, capitalizing on past development efforts and organizational expertise. Mechatronic system modifications often are limited to inexpensive control design changes, avoiding costly physical system changes. At times, the new system application requirements cannot be met through control changes alone. When this occurs requirements must be relaxed or physical system modifications must be considered. In the latter case, changes must be identified that satisfy requirements at minimum cost. A formal methodology for identifying candidate plant modifications and using co-design to minimize plant modification cost, known as PLCD, was introduced recently by Allison [10]. In Ref. [10], a robotic manipulator design problem was considered where the simplified plant design consisted only of link lengths and cross-section radii. Here a more sophisticated physical system is considered. Counterbalance masses help reduce joint torques and provide more design flexibility and potential for reduced energy consumption. This expanded plant design problem aids more complete exposition of the PLCD process, including new elements of sensitivity analysis.

1.1 Energy-Efficient Robotic Manipulator Design.

Robotic manipulators are ubiquitous in modern manufacturing; improved performance and energy efficiency can have important economic and environmental impact (see Li and Bone [11] and Spong et al. [12]). As identified by Field and Stepanenko [13], early manipulator design efforts were focused primarily on reducing task time, while recent work has concentrated more on energy efficiency improvement. Energy consumption is especially important for

[1]Corresponding author.

Contributed by the Mechanisms and Robotics Committee of ASME for publication in the JOURNAL OF MECHANICAL DESIGN. Manuscript received May 15, 2012; final manuscript received June 1, 2013; published online August 7, 2013. Assoc. Editor: James Schmiedeler.

mobile robotics (see Ahmadi and Buehler [14], Barili et al. [15], Mei et al. [16,17], Ooi and Schindelhauer [18], and Grieco et al. [19]), and techniques learned from these studies, such as trajectory design [16–18] and use of passive dynamics (e.g., Ahmadi and Buehler [14] or Pitti and Lungarella [20]), often can be extended to manipulator design (see Field and Stepanenko [13], Sarkar and Podder [21], Mattila and Virvalo [22], and Sato et al. [23]).

Manipulator counterbalance mechanisms (see Agrawal et al., Agrawal and Fattah, and Fattah and Agrawal [24–26]), such as springs or countermasses, can help reduce joint torques and energy consumption. As demonstrated by Tepper and Lowen [27], gravity-balanced manipulators can be designed such that the net torque at each joint in any position is zero under static conditions. Chung and Cho developed a mechanism and control policy for automatically adjusting the distance between counterweights and joints to accommodate a range of payloads [28], and Lim et al. investigated potential payload capacity increase using counterbalance mechanisms [29].

Cancellation of gravity forces produces near minimal energy consumption for slow movements. When motions are fast, however, dynamic effects increase joint torque requirements due to large counterweight masses (see Lim et al. [29]). Gravity force cancellation is easy to design for, and this has been used often as a proxy plant design objective for energy minimization (e.g., Chung and Cho [28], Lim et al. [29], Coello et al. [30], and Ravichandran et al. [31]). While using this proxy plant objective simplifies physical system design, in most cases the resulting systems are suboptimal and do not use minimal energy. This suboptimality is especially pronounced for high-acceleration applications, but can be ameliorated via innovative designs that cancel rotational inertia, such as the counter-rotary countermass mechanisms introduced by van der Wijk and Herder [32].

Developing robotic manipulators that consume minimal energy while performing practical (i.e., not pseudostatic) industrial tasks demands a more integrated design approach that accounts for physical dynamics. One strategy is to exploit the passive dynamics of a physical system to help perform the desired task. This strategy, which is often exhibited in biological systems, has been an inspiration for energy-efficient bio-mimetic systems. For example, McGeer introduced passive dynamic walkers that can walk down an incline powered only by gravitational potential energy and without any active joint control [33]. Collins et al. showed that adding small power sources to replace the force of gravity can enable similar walkers to move on level ground or up inclines with energy efficiency that is magnitudes better than conventional humanoid robots and comparable to the efficiency of human walking [34]. Carefully designed active control can work in concert with passive dynamics when the passive system alone cannot perform the desired task [14,35,36]. This approach can work well for optimizing energy efficiency or other performance metrics when passive dynamics are aligned with the desired task. If there is misalignment (e.g, slower time constants), control design alone is insufficient and plant redesign should be considered.

When passive dynamics or energy efficiency of actively controlled systems is addressed in the literature, often the focus is on control system design. Co-design offers a more comprehensive approach for developing a system design tailored for a specific task (or set of tasks); passive dynamics may be adapted via plant design to capitalize on synergy between physical and control system design and produce superior system performance. While mechatronic design is often approached in an integrated manner, application of co-design to robotic systems has been limited. Ravichandran et al. applied co-design to energy minimization of a counterbalanced manipulator, but used gravity balance as a proxy objective, resulting in a modified sequential process [31]. Park and Asada applied co-design to a manipulator, but used simplified system performance metrics, such as settling time [37].

In this article, an integrated co-design method is applied for the first time to counterbalanced robotic manipulator design, where the single system objective of energy efficiency based on nonlinear dynamic simulation is applied consistently across both plant and control design. Co-design is used here for several tasks; first, it is used to develop a baseline manipulator design that is optimized for an initial task (task A), and then it is used as part of the PLCD process to demonstrate how to adapt an existing system to perform a new task (task B) that was unanticipated when the baseline system was designed. Section 2 provides an overview of PLCD, Sec. 3 introduces the manipulator example problem and illustrates how to use co-design to produce the minimum-energy baseline design for task A, and Sec. 4 demonstrates how the PLCD process can be applied to redesign the manipulator for a new task. Results are discussed in Sec. 5, followed by concluding remarks.

2 Plant-Limited Co-Design

As introduced in Ref. [10], PLCD is a systematic process for repurposing mechatronic systems to meet requirements of a new application at minimal cost, consisting of four steps:

(1) Identify candidate plant modifications,
(2) develop a suitable system model,
(3) formulate and solve the PLCD optimization problem, and
(4) verify result and repeat if required.

In the first step, we analyze the system to determine which aspects of the plant we should modify. One approach for making this selection is to compute sensitivities that estimate which plant modifications will have the largest impact on system performance. Normally at this stage only a model suitable for control design is available, i.e., a model that cannot accommodate plant design changes. The second PLCD step expands the system model so that it can predict the effect of limited plant changes. When the model is complete we can formulate and solve the PLCD optimization problem (step 3). After we arrive at a solution we can verify whether further improvement can be achieved by altering the set of candidate plant modifications (step 4). If this is the case, the process can be repeated. These steps are described in more detail below.

2.1 Selecting Candidate Plant Modifications. While plant modifications in this article are limited to continuous geometric changes of existing components, they could include topological changes such as the addition, removal, or reconfiguration of components. We are interested in which candidate plant modifications have the greatest influence on requirements for the new system task that were violated when attempting to use the original plant design with updated control design. Reducing the number of candidate plant modifications helps limit plant modification cost, ease plant model modification effort, and can also reduce the difficulty of solving the PLCD optimization problem.

If the complete set of requirements for the new task is $\mathbf{g_r}(\mathbf{p}) \leq \mathbf{0}$, the subset of requirements the original system design is unable to meet (via control redesign alone) is denoted by $\bar{\mathbf{g}}_\mathbf{r}(\mathbf{p}) \leq \mathbf{0}$. $\mathbf{p}$ are system model parameters that depend on plant design variables $\mathbf{x_p}$. We compute the sensitivity of violated constraints with respect to plant design variables if a more complete plant model is available that maps design variables to model parameters, and with respect to $\mathbf{p}$ if not. The rationale here is to identify elements of plant design with the ability to influence system performance as efficiently as possible. Here the following sensitivity calculation is used to estimate this influence

$$\frac{\partial \bar{g}_{ri}(\mathbf{p})}{\partial p_j}, \quad i = 1, 2, \ldots, n_r, \quad j = 1, 2, \ldots, n_p \tag{1}$$

where n_r is the number of violated constraints and n_p is the number of model parameters. These terms form the model parameter Jacobian $\mathbf{J}_p$. Requirement i is influenced significantly by small changes in p_j if the magnitude of $\partial \bar{g}_{ri}(\mathbf{p})/\partial p_j$ is large. After a set

of influential model parameters $\bar{\mathbf{p}}$ is identified based on $\mathbf{J}_p$, a corresponding set of candidate plant changes $\bar{\mathbf{x}}_\mathbf{p}$ that influence $\bar{\mathbf{p}}$ must be established. Note that $\bar{\mathbf{x}}_\mathbf{p}$ is a subset of variables selected from the full set of plant design variables $\mathbf{x}_\mathbf{p}$ that corresponds to complete system redesign. The system model can then be expanded based on $\bar{\mathbf{x}}_\mathbf{p}$, as described in the next step.

If a cost model is available, a more sophisticated analysis for selecting $\bar{\mathbf{x}}_\mathbf{p}$ can be performed that involves the sensitivity of violated requirements with respect to the cost of parameter changes. Suppose a cost model has been developed that expresses plant modification cost as a function of model parameters, i.e., $C(\mathbf{p})$. This model may be used to identify which parameters influence system requirements most strongly at the lowest modification cost. To do this, the Jacobian terms in Eq. (1) are scaled using the derivative of cost with respect to parameter changes to obtain $\partial \bar{g}_{ri}(\mathbf{p})/\partial c_j$, which quantifies how sensitive requirement i is to the cost of changing parameter j (i.e., c_j). This sensitivity is calculated as follows:

$$\left(\frac{\partial \bar{g}_{ri}(\mathbf{p})}{\partial p_j}\right)\left(\frac{\partial C(\mathbf{p})}{\partial p_j}\right)^{-1} = \frac{\partial \bar{g}_{ri}(\mathbf{p})}{\partial c_j}, \quad \begin{matrix} i = 1,2,\ldots,n_r \\ j = 1,2,\ldots,n_p \end{matrix} \tag{2}$$

The $\partial \bar{g}_{ri}(\mathbf{p})/\partial c_j$ terms form the cost Jacobian $\mathbf{J}_c$, which can be used to assess which plant modifications could produce the desired performance improvements most economically.

Sensitivity analysis is inherently local, and in some cases may not lead to the best set of candidate plant modifications. Other more sophisticated methods, such as change propagation analysis [38,39], should be explored as alternative strategies for identifying candidate plant modifications. That said, sensitivity analysis was shown through enumeration to identify the optimal set of candidate plant modifications for the case study presented in Ref. [10].

While sensitivity calculation is presented as a component of the larger PLCD process, it may be used alone in conjunction with conventional design methods. For example, once $\bar{\mathbf{x}}_\mathbf{p}$ is identified using sensitivity analysis, engineers can proceed using conventional design methods to modify the plant and then the control system in a sequential manner. This may be sufficient, and the relatively small modeling and analysis investment is appealing, but will not result in a system-optimal design. If this simplified approach is not successful, the full PLCD process should be implemented. In addition, if one iteration of PLCD fails to identify a new design that satisfies requirements based on a particular $\bar{\mathbf{x}}_\mathbf{p}$, the criteria for selecting $\bar{\mathbf{p}}$ should be relaxed to increase the dimension of $\bar{\mathbf{x}}_\mathbf{p}$.

2.2 System Model Development. Solving the PLCD optimization problem described in step 3 requires a system model that has as independent variables the candidate plant modifications $\bar{\mathbf{x}}_\mathbf{p}$ identified in step 1. Models that predict accurately the results of physical system design changes are challenging to develop, often requiring significant resource investment. Developing a system model that accommodates all possible plant changes is unnecessary (and often impractical) for PLCD problems; reducing the number of candidate plant changes identified in step 1 is important for curbing model development expense and easing optimization solution difficulty.

One possible modeling approach is to augment the existing control design model used in step 1 with specialized models that predict model parameter values for a given $\bar{\mathbf{x}}_\mathbf{p}$. More precisely, we seek a model of the form $\mathbf{p} = \mathbf{a}(\bar{\mathbf{x}}_\mathbf{p})$, where $\mathbf{a}(\bar{\mathbf{x}}_\mathbf{p})$ is an analysis function that computes model parameters as a function of independent plant design variables using computer aided engineering tools such as finite element analysis. This system model structure for co-design was described by Allison and Nazari [40].

Reducing the dimension of $\mathbf{x}_\mathbf{p}$ via sensitivity analysis or other means is similar in nature to model order reduction [41], but instead of reducing state space dimension we seek to reduce design space dimension. In addition, the objective in model order reduction is to reduce the complexity of an existing model; whereas, here the objective is restrict model dimension a priori. Techniques for a posteriori design model reduction exist, such as monotonicity analysis [42], but strategies for the a priori design model dimension reduction required in PLCD is an opportunity for future work. Note that *design* model dimension reduction refers to identification of plant design variables to hold fixed, which is different from model order reduction where the number of states in a model is reduced. Model order reduction has a rich literature, whereas, a priori design model dimension reduction is a relatively new topic that is important for PLCD.

2.3 PLCD Problem Formulation and Solution. With a reduced set of candidate plant modifications $\bar{\mathbf{x}}_\mathbf{p}$ and a corresponding plant model now available, the PLCD problem can be formulated as a design optimization problem and solved. Consider the following PLCD optimization problem

$$\begin{aligned} \min_{\mathbf{x}=\left[\bar{\mathbf{x}}_\mathbf{p}^\mathrm{T},\mathbf{x}_\mathbf{c}^\mathrm{T}\right]^\mathrm{T}} \quad & \phi(\mathbf{x}) \\ \text{s.t.} \quad & \mathbf{g}_\mathbf{p}(\mathbf{x}) \le 0 \\ & \mathbf{g}_\mathbf{r}(\mathbf{x}) \le 0 \end{aligned} \tag{3}$$

where $\phi(\mathbf{x})$ is a measure of deviation from the original plant design, $\mathbf{g}_\mathbf{p}(\mathbf{x})$ are plant design constraints, and $\mathbf{g}_\mathbf{r}(\mathbf{x})$ are system performance requirements formulated as inequality constraints. Both sets of constraints are assumed to be predefined here. Note that $\mathbf{g}_\mathbf{r}(\mathbf{x})$ represents the full set of system requirements, not just the violated constraints used in step 1 for identifying candidate plant modifications. In addition, because a new objective function $\phi(\mathbf{x})$ is introduced, the original design objective may be recast as a constraint to ensure adequate performance. The optimization variable $\bar{\mathbf{x}}_\mathbf{p}$ parametrizes the candidate plant modifications, and $\mathbf{x}_\mathbf{c}$ are the control design variables. The solution to this problem is a system design that meets performance requirements while requiring minimal modifications to the physical system design.

Several options exist for constructing the metric $\phi(\mathbf{x})$. It could be a simple weighted norm that penalizes moving away from the original design $\mathbf{x}_\mathbf{0}$ (e.g., $\phi(\mathbf{x}) = \|\mathbf{w} \circ (\mathbf{x}_\mathbf{0} - \mathbf{x}_\mathbf{p})\|$), or more ideally a cost model that predicts accurately the cost of changing the plant design [43,44]. In the case study here, the cost of plant changes is approximated using component-wise change in mass

$$\phi(\mathbf{x}) = \sum_{i=1}^{n_c} |m_i(\mathbf{x}) - \hat{m}_i| \tag{4}$$

where n_c is the number of plant components being modified, $m_i(\mathbf{x})$ is the mass of component i based on the modified design $\mathbf{x}$, and $\hat{m}_i$ is the mass of component i in the baseline design. This approximates, in a very simple manner, the cost of limited plant redesign to the manufacturer. A more complete study would include full lifecycle cost, including use (such as energy and maintenance costs) and end-of-life costs, a subject of current work. Multi-objective optimization may also be performed to explore the tradeoff between cost and system performance for the new application. This tradeoff will be investigated for the counterbalanced robotic manipulator problem presented here.

3 Energy Minimization Using Co-Design

A two-link planar manipulator was selected to demonstrate the PLCD solution process. This manipulator is similar to the one used in Ref. [10], but incorporates a counterbalance mechanism that helps to reduce energy consumption further. This topological change also provides greater opportunity for plant design modifications, which is useful for exposition of the PLCD methodology. The manipulator used here, shown in Fig. 1(*a*), has two mechanical degrees of freedom (joint angles θ_1 and θ_2), and is designed to

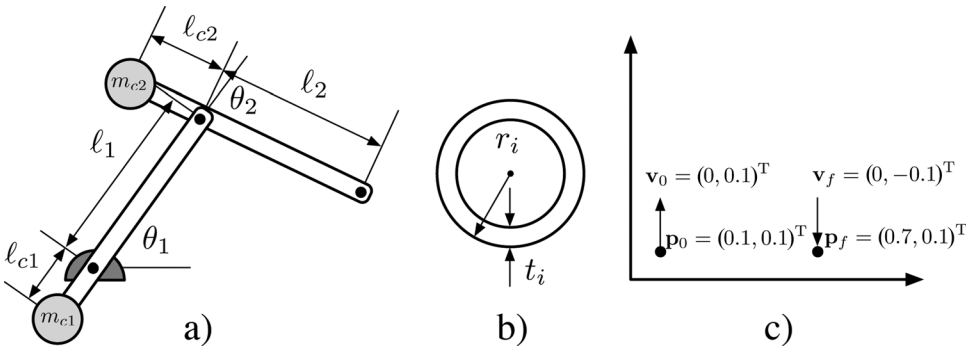

Fig. 1 (*a*) Counterbalanced two-link planar manipulator, (*b*) section view of link *i*, and (*c*) task A initial and final conditions

move a payload at the end effector for a pick-and-place task. While other manipulator configurations are typically chosen for this type of operation in practice, this combination of configuration and task has proven especially useful for investigating PLCD.

Links 1 and 2 are counterbalanced by masses m_{c1} and m_{c2}, respectively, with gravity directed downward. Here we do not assume these masses or their offset distances (ℓ_{c1} and ℓ_{c2}, respectively) are chosen such that gravity forces cancel out. Designs without perfect gravity balance may be more desirable due to dynamic effects. Please note that allowing designs with imperfect balance does not preclude the possibility of perfectly balanced design solutions. The objective here is to minimize energy consumption, and the optimization approach will identify the design that does this, regardless of whether the design is balanced or not.

Each link has a constant cross section depicted by Fig. 1(*b*) with radius r_i and wall thickness t_i. The complete plant design vector is

$$\mathbf{x_p} = [\ell_1, \ell_2, \ell_{c1}, \ell_{c2}, m_{c1}, m_{c2}, r_1, r_2]^{\mathrm{T}}$$

To demonstrate PLCD, a baseline manipulator design is needed. Limited redesigns will then be derived from this baseline design using PLCD. The baseline manipulator design will be obtained by using co-design to minimize energy consumption for the initial manipulator task (task A). In addition, a "nominal" design will be developed using a sequential design method for the purpose of illustrating the value of co-design. The baseline design (i.e., the co-design result) will be shown to consume far less energy the nominal design (i.e., sequential design result). Next, a new task will be introduced (task B). First, co-design will be applied to obtain a "clean-sheet" design for task B, i.e., the complete system will be redesigned from scratch. It will be seen that the clean-sheet redesign has very low energy consumption when performing task B, but requires a completely different plant design, so is a very high-cost option. PLCD is then applied to redesign the baseline design for task B in a limited fashion, both for minimum modification cost and minimum energy. Finally, a study is performed that illustrates the tradeoff between energy efficiency and plant modification cost.

3.1 Co-Design Formulation. The manipulator design problem is formulated here as a simultaneous co-design problem where $\mathbf{x_p}$ and $\mathbf{x_c}$ are sought that minimize the energy $E(\mathbf{x})$ consumed while performing a specified task, while satisfying torque (τ) and link deflection (δ) constraints

$$\begin{aligned} \min_{\mathbf{x}=[\mathbf{x_p},\mathbf{x_c}]} \quad & E(\mathbf{x}) \\ \text{s.t.} \quad & \max(|\tau_i(\mathbf{x}, t)|) \le \tau_{\text{allow}}, \quad i=1,2 \\ & \delta_i(\mathbf{x_p}) \le \delta_{\text{allow}}, \quad i=1,2 \end{aligned} \tag{5}$$

The maximum absolute torque value $\max(|\tau_i(\mathbf{x}, t)|)$ for each of the two joints must not exceed the allowable joint torque τ_{allow}, and the maximum deflection of each link $\delta_i(\mathbf{x_p})$ must not exceed the allowable deflection value δ_{allow}. These two sets of constraints are the design requirements for both the baseline design and the redesign developed using PLCD. The torque constraints are due to actuator limits, and the deflection constraints ensure structural integrity and the validity of the rigid-body dynamic model described below.

The initial task (task A) involves moving a 20 kg payload from the initial position $\mathbf{p}_0$ with initial velocity $\mathbf{v}_0$, and $t_f = 2.0$s later place the payload at $\mathbf{p}_f$ with final velocity $\mathbf{v}_f$ (Fig. 1(*c*)). Note that this task is not a complete cycle, so the energy calculated here is not indicative of energy requirements for continuous operation.

The desired (quintic) trajectory for the joint angular positions $\mathbf{q_d}(t) = [\theta_1(t), \theta_2(t)]^{\mathrm{T}}$ is calculated based on the task end conditions, as well as the position $\mathbf{p}_I$ and velocity $\mathbf{v}_I$ of an intermediate point along the path between $\mathbf{p}_0$ and $\mathbf{p}_f$. The intermediate point parameterizes the trajectory, and is a design decision to be made in solving Prob. (5).

Feedback linearization with a Proportional Derivative (PD) controller was used initially to track $\mathbf{q_d}(t)$ [12], but it was found that inverse dynamics—i.e., calculating joint torque trajectories as a function of $\mathbf{q_d}(t)$ using the equations of motion given in Eq. (6)—resulted in very little torque or energy consumption error compared to forward simulation with feedback linearization. Inverse dynamics was adopted for the design studies presented here, and had two important effects. First, it reduced the dimension of the control design vector because $\mathbf{u}(t)$ may be computed (approximately) without the PD control gains K_P and K_D. The reduced-dimension control design vector consists only of the trajectory parameters

$$\mathbf{x_c} = [p_{I1}, p_{I2}, v_{I1}, v_{I2}]^{\mathrm{T}}$$

Second, computational expense is significantly lower when using inverse dynamics since feedback linearization requires forward simulation. The reduced problem dimension and reduced function evaluation time due to inverse dynamics combine to ease optimization difficulty.

Low error between inverse dynamics and feedback linearization is expected when the actively controlled system moves at a speed that is similar to or slower than passive system dynamics. Shorter task times would increase this error. In addition, the inclusion of sensor or actuator dynamics at later design stages where more model detail is required may also increase this error, requiring the use of forward simulation.

It is assumed here that no energy is recovered under forward or reverse braking conditions (i.e., no regenerative braking; see Refs. [13–15] for other examples of this assumption for robotic systems). Maximum link deflection was calculated using standard beam formulas with a nominal joint torque applied as detailed in Ref. [10]. Note that only link deflection is considered here. While

joint deflection is often significant, it is not included in this simplified model. The link deflection constraint can be shown to be active [42], allowing solution for required radius values and elimination of radii from $\mathbf{x_p}$ via substitution, resulting in a reduced-dimension plant design vector

$$\mathbf{x_p} = [\ell_1, \ell_2, \ell_{c1}, \ell_{c2}, m_{c1}, m_{c2}]^{\mathrm{T}}$$

The following nonlinear differential equation, detailed in Ref. [12], was used to model manipulator dynamics

$$\mathbf{M}(\mathbf{q}, \mathbf{x_p})\ddot{\mathbf{q}} + \mathbf{C}(\mathbf{q}, \dot{\mathbf{q}}, \mathbf{x_p})\dot{\mathbf{q}} + \mathbf{g}(\mathbf{q}, \mathbf{x_p}) = \boldsymbol{\tau} \tag{6}$$

where $\mathbf{M}(\mathbf{q}, \mathbf{x_p})$ is the inertia matrix, $\mathbf{C}(\mathbf{q}, \dot{\mathbf{q}}, \mathbf{x_p})$ represents centrifugal and Coriolis terms, and $\mathbf{g}(\mathbf{q}, \mathbf{x_p})$ is the gravity vector. The joint torque vector is $\boldsymbol{\tau} = [\tau_1, \tau_2]^{\mathrm{T}}$, and corresponds to the control input in this example problem. Energy consumption is calculated by integrating mechanical power at each joint (neglecting power generated during braking). Complete details of this model are provided via published MATLAB® code [45].

In this model, a number of simplifications have been made. The example problem has been tailored in a way that allows clear investigation and explication of core PLCD issues. For example, the manipulator links are assumed to be rigid in the dynamic model. Rigid-body models are far simpler than those that account for structural dynamics. While joint motor mass and rotational inertia may be significant factors in the dynamic behavior of manipulators like the one considered here, both actuator and sensor dynamics have been neglected. These model simplifications help reduce problem dimension and enable detailed discussion of the example problem results. This simplified model, however, still retains important properties that are important for investigating PLCD, such as the effect of mass distribution on dynamics and synergy between plant and control design.

Another vital characteristic that is retained in this model is the dependence of dynamic performance on independent plant design variables. Models with this property can accommodate plant design changes, which is essential for co-design studies. More often, dynamic system models are based directly on parameters $\mathbf{p}$ that depend on plant design ($\mathbf{p}$ are not independent design variables). Establishing the dependence of $\mathbf{p}$ on $\mathbf{x_p}$ often requires significant modeling effort, so, as described above, it is desirable in PLCD to limit the scope of plant redesign.

To clarify the relationship between model parameters and plant design variables, consider a standard linear time-invariant system model: $\dot{\boldsymbol{\xi}} = \mathbf{A}(\mathbf{p})\boldsymbol{\xi} + \mathbf{B}(\mathbf{p})\mathbf{u}$, where $\boldsymbol{\xi}$ is the state vector and $\mathbf{u}$ is the control input. Components of system matrix $\mathbf{A}(\cdot)$ depend on time-invariant system parameters $\mathbf{p}$. For example, the system matrix in the active suspension co-design problem given in Ref. [46] includes terms, such as $a_{21} = 4k_t/m_{us}$, that depend on system parameters (e.g., tire stiffness k_t and unsprung mass m_{us}). These parameters are not independent design variables; they depend in a complicated way on independent design variables such as tire geometry. If a model of this dependence is not known for a PLCD problem, then $\mathbf{p}$ may be used directly in the sensitivity analysis, after which the relationship between $\mathbf{p}$ and the reduced set of candidate plant design variables $\bar{\mathbf{x}}_\mathbf{p}$ must be established.

In the nonlinear system model described in Eq. (6), the components of $\mathbf{M}(\cdot), \mathbf{C}(\cdot)$, and $\mathbf{g}(\cdot)$ depend on both plant design and system state. While not expressed explicitly in the model above, intermediate parameters are involved in these dependence relationships. For example, some components of $\mathbf{M}(\cdot)$ involve moments of inertia for links 1 and 2, which in turn depend on link geometry defined by $\mathbf{x_p}$. These inertia quantities are elements of $\mathbf{p}$ in the manipulator example, but are not used in the PLCD sensitivity analysis because model dependence on $\mathbf{x_p}$ is known and $\mathbf{x_p}$ may be used directly.

Full development and implementation of a manipulator would require a notably more sophisticated design model with greater geometric detail, more realistic component models, feedback control architecture design, and tests involving a more comprehensive set of manipulation tasks. That said, the co-design model presented here offers a deeper treatment of physical system design than much of the co-design literature, as it includes independent plant design variables, physics-based plant constraints, and a nonlinear system model. Ongoing work—outside the scope of this article—is addressing mechatronic system co-design based on high-fidelity models, including the use of emerging techniques such as derivative function surrogate modeling to enable the optimization of nonlinear dynamic systems that involve computationally intensive simulations [47].

3.2 Nominal Manipulator Design. As described above, a nominal manipulator design was developed, based on sequential design, to illustrate the value of using co-design. In the first phase of this sequential process, a plant design was developed that is kinematically capable of executing task A ($\mathbf{x_p} = [1.0, 1.0, 0.3, 0.3, 10, 10]^{\mathrm{T}}$). Then, an optimal trajectory was computed for this plant design that minimizes energy consumption (i.e., Prob. (5) was solved with respect to $\mathbf{x_c}$ with $\mathbf{x_p}$ held fixed). This nominal design consumes 27.6 J when performing task A; the corresponding trajectories are illustrated in Fig. 2. The payload is lifted up from $\mathbf{p}_0$ and set down at $\mathbf{p}_f$ (Fig. 2(*a*)). Here the maximum torque bound limit was 210 Nm, which was reached by τ_1 (Fig. 2(*b*)). The starting point of the trajectories is indicated with a circle.

3.3 Baseline Optimal Manipulator Design. The system-optimal baseline design for task A was generated by solving the co-design problem that is detailed in Prob. (5) (with $\tau_{\mathrm{allow}} = 160$ Nm), reducing energy consumption to essentially *zero* for task A ($E = 5.86 \times 10^{-5}$ J). The payload follows a similar path (Fig. 3) to the nominal design, but the new mass

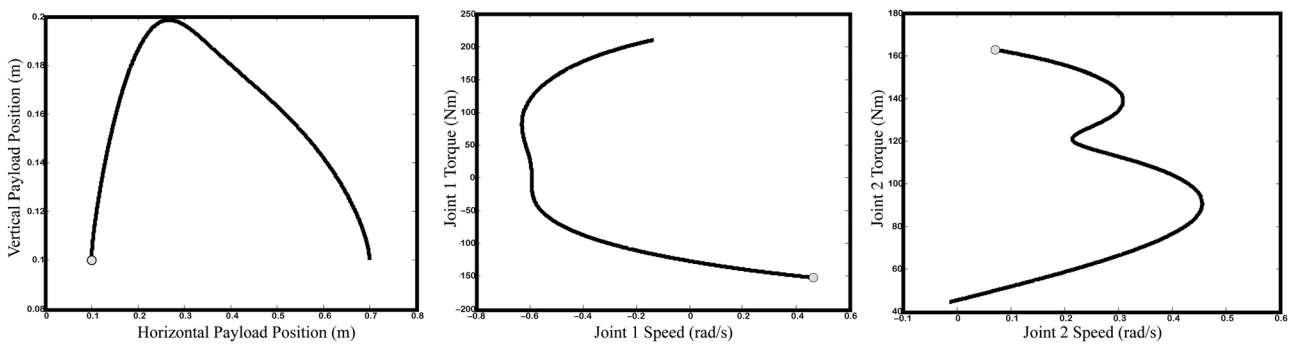

Fig. 2 Optimal trajectories for nominal plant design: (*a*) Payload trajectory, (*b*) joint 1, and (*c*) joint 2 torque-speed trajectories

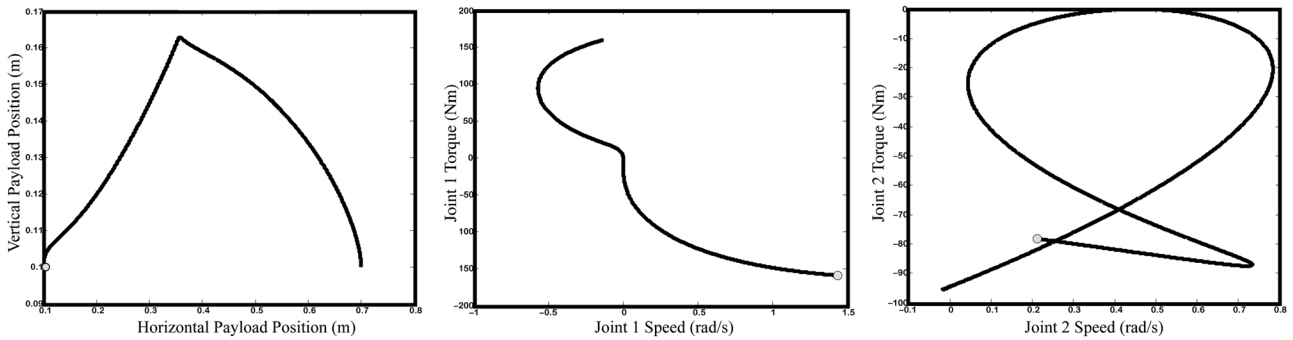

Fig. 3 Task A co-design results: (*a*) Payload trajectory, (*b*) joint 1, and (*c*) joint 2 torque-speed trajectories

distribution allows for torque-speed trajectories that are significantly different. Torque curves for both joints remain in either the forward or reverse braking quadrants (i.e., $\tau \times \omega \leq 0$), so (approximately) no power is consumed. This result is similar to the design strategy used by Arai and Taichi, who combined actively controlled joints and joints with only braking capability to design a manipulator that could perform tasks similar to those used in this article [48]. Recall that here we assume no braking energy can be recovered (i.e., energy is dissipated as heat during braking), so negative power under braking does not contribute to the energy consumption metric. The optimal baseline design is

$$\mathbf{x_p} = [0.838, 0.711, 0.216, 0.885, 3.89, 20.7]^{\mathrm{T}}$$

$$\mathbf{x_c} = [0.359, 0.163, 0.00829, -0.0249]^{\mathrm{T}}$$

The link lengths are significantly shorter than those presented in Ref. [10] for the same task. The counterbalance mechanism enables shorter arms to attain the correct passive dynamics that allow task A completion with only joint braking. In Ref. [10], however, torque trajectories were near zero during much of the simulation, indicating significant utilization of passive dynamics. The manipulator in Ref. [10] was not counterbalanced and required nonbraking torque and more energy to perform task A.

4 Plant-Limited Co-Design of a Robotic Manipulator

The co-design result of Sec. 3.3 serves as a baseline design for demonstrating PLCD. Here we introduce a new task (task B) that the manipulator is to perform, ideally with very limited changes. The new task is specified by the following end conditions:

$$\mathbf{p}_0 = [0.5, 1.2]^{\mathrm{T}}\mathrm{m}, \quad \mathbf{v}_0 = [-0.1, 0]^{\mathrm{T}}\mathrm{m/s},$$

$$\mathbf{p}_f = [0.4, 2.0]^{\mathrm{T}}\mathrm{m}, \quad \mathbf{v}_f = [-0.1, 0]^{\mathrm{T}}\mathrm{m/s}$$

In task A, the payload vertical position did not change between end conditions, but here it increases by 0.8 m, raising the gravitational potential energy of the payload by

$$(20\ \mathrm{kg}) \times (9.81\ \mathrm{m/s^2}) \times (0.8\ \mathrm{m}) = 157\ \mathrm{J}$$

Observing the link lengths from the task A design, the maximum extension of the manipulator is $0.838 + 0.711 = 1.549$ m, and is unable to perform task B due to kinematic restrictions ($\mathbf{p}_f$ is unreachable: $\|\mathbf{p}_f\| = 2.040\ \mathrm{m} > 1.549\ \mathrm{m}$). In the PLCD example given in Ref. [10], the task A design was kinematically (but not dynamically) capable of performing task B. This new complication of kinematic infeasibility allows explication of new plant redesign techniques.

4.1 Task B Co-Design. Before proceeding with the identification of $\bar{\mathbf{x}}_\mathbf{p}$ for task B and PLCD optimization, a clean-sheet design is developed for cost comparison with limited redesign. In clean-sheet design for task B, Prob. (5) is solved with a complete set of plant design variables ($\mathbf{x_p}$), i.e., co-design is used to redesign completely the manipulator for task B. This represents the best possible design for task B if cost was not a concern. The task B co-design result is

$$\mathbf{x_p} = [1.69, 0.947, 2.46, 0.708, 28.2, 29.6]^{\mathrm{T}}$$

$$\mathbf{x_c} = [0.499, 1.46, -0.593, -0.125]^{\mathrm{T}}$$

and $E = 1.56 \times 10^{-4}$J (again, essentially zero). Near-zero energy consumption is possible even when the payload is moved vertically 0.8 m because the mass center of the manipulator–payload system is actually lower at the end of task B than at the beginning, owing to a well-designed counterbalance mechanism.

Figure 4 illustrates the trajectories of the task B co-design result. As with task A co-design, the torque-speed trajectories are always either in the forward or reverse braking quadrants. Neither joint actuator reaches the torque bound of 160 Nm, so it would be possible to reduce actuator size further in this case. The approximate plant modification cost, based on mass change and given by Eq. (4), for task B co-design is 121 kg.

In the next step, a limited set of plant design modifications will be identified that allow the satisfaction of task B requirements at much lower cost than 121 kg.

4.2 Sensitivity Analysis. PLCD sensitivity analysis would normally be performed by using the task A plant design to perform task B (with optimal trajectories and control). An alternate approach must be used here because the original design is kinematically incapable of performing task B. The set of requirements ($\mathbf{g_r}(\mathbf{p}) \leq \mathbf{0}$) that are violated for task B is undefined because the baseline design cannot perform task B. The sensitivity is instead obtained for all performance metrics (i.e., E and $\tau_{\max}$) based on task A simulation to approximate which design variables have the greatest impact on improving the system design for task B. For greater accuracy, once a design that is kinematically feasible for task B is obtained by completing one or more PLCD iterations, a sensitivity analysis based on task B simulation may be used to help identify an improved set of candidate plant modifications.

After computing the sensitivities of energy consumption and the torque constraints with respect to the complete plant design vector (using optimal trajectories for each calculation), the cost model given in Eq. (4) was combined with these values to compute the cost Jacobian defined in Eq. (2). Here the magnitude of each component is given

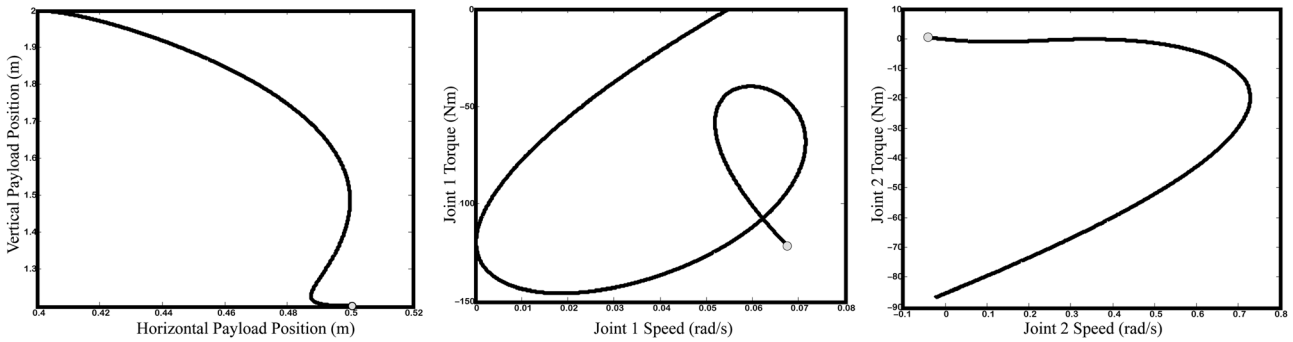

Fig. 4 Task B co-design results: (*a*) Payload trajectory, (*b*) joint 1, and (*c*) joint 2 torque-speed trajectories

$$\mathbf{J_c} = \begin{bmatrix} \frac{\partial E(\mathbf{p})}{\partial c_1} & \frac{\partial E(\mathbf{p})}{\partial c_2} & \frac{\partial E(\mathbf{p})}{\partial c_3} & \frac{\partial E(\mathbf{p})}{\partial c_4} & \frac{\partial E(\mathbf{p})}{\partial c_5} & \frac{\partial E(\mathbf{p})}{\partial c_6} \\ \frac{\partial g_{r1}(\mathbf{p})}{\partial c_1} & \frac{\partial g_{r1}(\mathbf{p})}{\partial c_2} & \frac{\partial g_{r1}(\mathbf{p})}{\partial c_3} & \frac{\partial g_{r1}(\mathbf{p})}{\partial c_4} & \frac{\partial g_{r1}(\mathbf{p})}{\partial c_5} & \frac{\partial g_{r1}(\mathbf{p})}{\partial c_6} \\ \frac{\partial g_{r2}(\mathbf{p})}{\partial c_1} & \frac{\partial g_{r2}(\mathbf{p})}{\partial c_2} & \frac{\partial g_{r2}(\mathbf{p})}{\partial c_3} & \frac{\partial g_{r2}(\mathbf{p})}{\partial c_4} & \frac{\partial g_{r2}(\mathbf{p})}{\partial c_5} & \frac{\partial g_{r2}(\mathbf{p})}{\partial c_6} \end{bmatrix}$$

$$= \begin{bmatrix} 3.26 & 0.0023 & 0.143 & 0.0034 & 0.0155 & 0.0193 \\ 0.0125 & 0.0334 & 0.0129 & 0.0007 & 0.694 & 0.0028 \\ 397 & 14.6 & 433 & 38.6 & 298 & 221 \end{bmatrix} \begin{matrix} \text{J/kg} \\ \text{Nm/kg} \\ \text{Nm/kg} \end{matrix}$$

4.3 Limited Plant Redesign. Kinematic feasibility must be considered when deciding which candidate plant modifications to include in the PLCD problem formulation. The total link length must be at least $\ell_1 + \ell_2 = 2.04$ m for $\mathbf{p}_f$ to be reachable; at least one of the link lengths must be included in the set of candidate plant modifications to satisfy this requirement. It is clear from column 1 of $\mathbf{J_c}$ that ℓ_1 is most influential. ℓ_{c1}, m_{c1}, and m_{c2}, corresponding to columns 3, 5, and 6, were also selected to form the vector of candidate plant design changes:

$$\bar{\mathbf{x}}_\mathbf{p} = [\ell_1, \ell_{c1}, m_{c1}, m_{c2}]^\mathrm{T}$$

The other two design variables were held fixed at the task A optimal design values. The selection $\bar{\mathbf{x}}_\mathbf{p}$ was made subjectively based on what variables had the greatest impact for the least cost, quantified by $\mathbf{J_c}$. While this subjective approach has proven successful for relatively small example problems, more formal selection methods will be required for larger PLCD problems, and is a subject for future work.

Two approaches were taken here for limited plant redesign. First, the original co-design problem given in Eq. (5) was solved with respect to the limited plant design vector. This alternative PLCD formulation does not minimize modification cost, but instead provides a lower bound on energy consumption for the limited plant redesign. The resulting modification cost is lower than with clean-sheet design since fewer components are modified. The second approach involves the solution of the PLCD optimization problem given in Prob. (3) to minimize plant modification cost. An upper bound on energy consumption was included: $E(\mathbf{x}) \leq 0.001$ J. The solutions of these two limited redesign problems are two points on a Pareto set that illustrates the tradeoff between modification cost and energy consumption; the solution to the first problem is the limited redesign that minimizes energy without regard to cost, while the solution to the second problem minimizes cost with stringent limits on energy consumption. Additional Pareto-optimal designs were obtained by relaxing the energy bound to further reduce modification cost (Fig. 5). This tradeoff information could be used to determine whether requirement relaxation may be worth the modification cost savings, as well as to demonstrate the importance of making plant modification in achieving requirements for the new system application.

Figure 6 illustrates the trajectories for the first solution that minimizes energy; this solution corresponds to the upper left point on the Pareto set in Fig. 5. As with other energy-minimizing designs, the torque-speed trajectories remain within the forward and reverse braking quadrants. The torque at joint 1 does hit the bound of 160 Nm. The corresponding system design is

$$\mathbf{x_p} = [1.61, 0.711, 0.126, 0.885, 15.7, 19.6]^\mathrm{T}$$

$$\mathbf{x_c} = [0.565, 1.48, -0.595, -0.173]^\mathrm{T}$$

Observe that the second and fourth plant design variables are at the same values as in the baseline design—they were held fixed for the limited redesign. The energy consumption here was 7.71×10^{-4} J, a small increase from the task B co-design result, but still essentially zero. The cost of these modifications using the approximate cost metric is 24.3 kg, significantly less than the cost of the task B co-design result (121 kg).

In the second solution approach, the value of PLCD is demonstrated by showing that plant modification cost can be reduced significantly with a relatively small increase in energy consumption. In this PLCD problem energy consumption was limited to 0.001 J, and Prob. (3) was solved to minimize modification cost. The minimum cost was 9.95 kg, 92% lower than the task B co-design result and 59% lower than PLCD with energy minimization. The corresponding system design is

$$\mathbf{x_p} = [1.56, 0.711, 0.363, 0.885, 3.89, 20.7]^\mathrm{T}$$

$$\mathbf{x_c} = [0.576, 1.51, -0.522, -0.288]^\mathrm{T}$$

Note that while two counterbalance masses are components of $\bar{\mathbf{x}}_\mathbf{p}$, they remained at their baseline values of 3.89 and 20.7 kg. This is due to using mass change as an approximate cost metric and the fact that most of the system mass is located in the counterbalance masses. As observed in the above solution, the desired counterbalance effect can be achieved without changing counterbalance masses by adjusting link geometry with relatively little mass penalty.

Figure 7 illustrates the trajectories for the PLCD with cost minimization where $E(\mathbf{x}) \leq 0.001$. Energy consumption is still very near zero. The manipulator operates almost exclusively in the forward and reverse braking quadrants, as with the other co-design results. In Figs. 4(*c*), 6(*c*), and 7(*c*), note that the joint two actuator does spend a significant portion of the simulation near zero torque, indicating that passive dynamics are utilized partially in these designs.

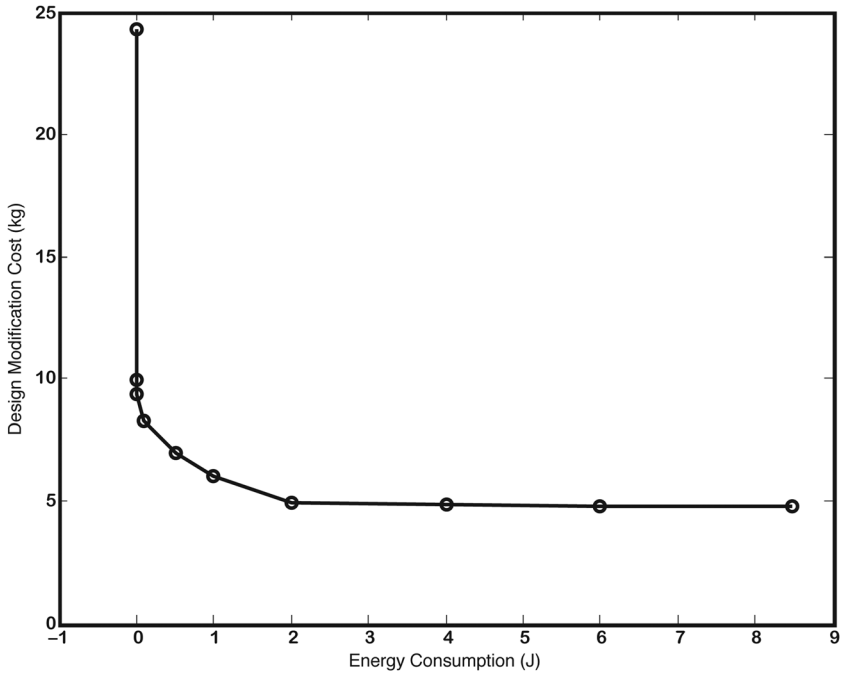

Fig. 5 Pareto set illustrating the tradeoff between energy consumption and plant redesign cost

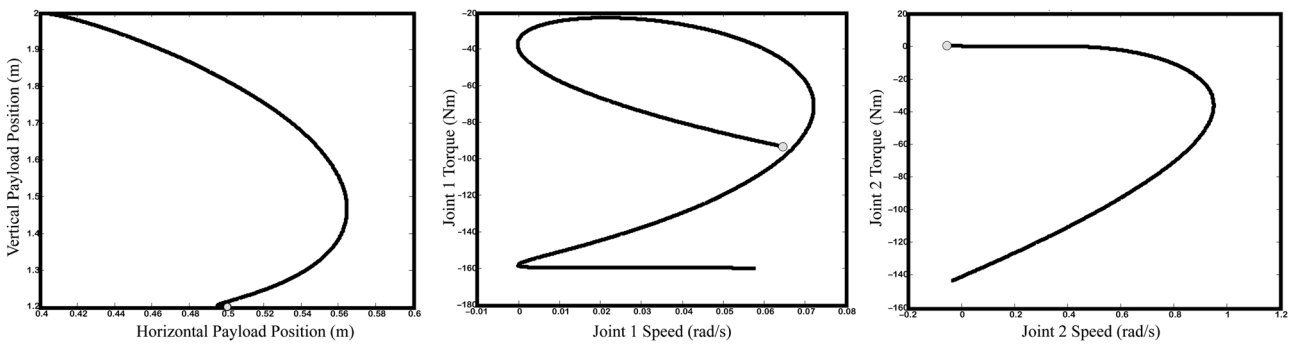

Fig. 6 Task B limited redesign results (min $E(\mathbf{x})$): (*a*) Payload trajectory, (*b*) joint 1, and (*c*) joint 2 torque-speed trajectories

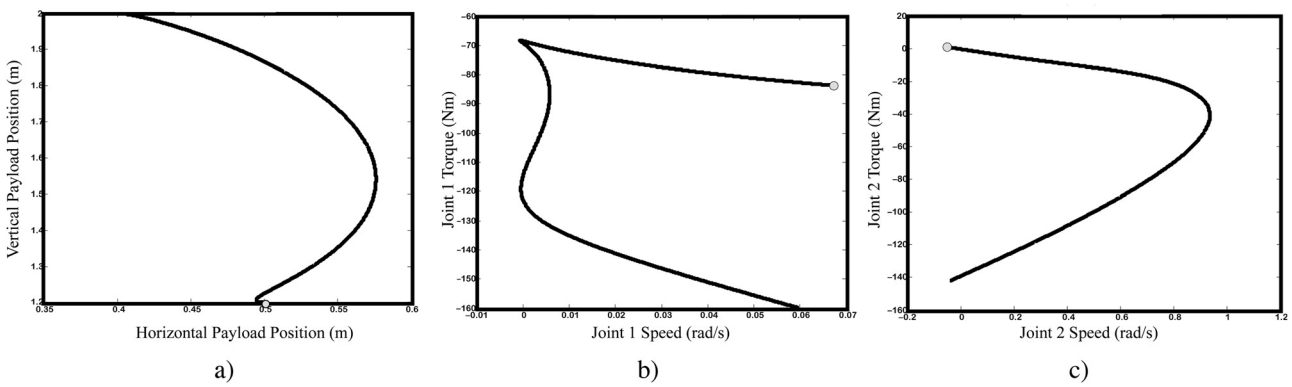

Fig. 7 Task B PLCD results ($E \leq 0.001$ J): (*a*) Payload trajectory, (*b*) joint 1, and (*c*) joint 2 torque-speed trajectories

Table1 summarizes the design results from the manipulator case study, illustrating the effectiveness of the PLCD methodology for reducing redesign cost while maintaining superior performance.

5 Discussion

PLCD is a recently introduced design methodology for repurposing mechatronic systems where limited plant modifications

Table 1 Summary of robotic manipulator design results

	Energy consumption (J)	Modification cost (kg)
Task A nominal $\mathbf{x_p}$, opt. $\mathbf{x_c}$	27.6	—
Task A co-design (baseline)	5.86×10^{-3}	—
Task B co-design	1.56×10^{-4}	121
Task B PLCD (min E)	7.71×10^{-4}	24.3
Task B PLCD ($E \leq 0.001$ J)	0.001	9.95
Task B PLCD ($E \leq 2.0$ J)	2	4.95

must be made to meet requirements. This challenging task arises frequently in practice, and engineers often struggle to adapt a system to new applications through control design changes alone. PLCD methodology provides a systematic approach for identifying influential candidate design variables and minimizing the cost of physical system design changes required to meet new application requirements. PLCD results provide quantitative justification for considering plant design modifications, and cost–performance tradeoff information can be obtained using multi-objective optimization. Applying co-design methodology to a ground-up system development project is challenging, and may be impractical in many current organizations. PLCD can be viewed as an intermediate step toward adopting co-design; it requires a lower level of commitment and investment, and solves a pressing nascent problem for firms that develop mechatronic systems.

PLCD was applied to the repurposing of a counterbalanced robotic manipulator. A baseline design for task A was developed using co-design, which successfully exploited passive system dynamics to reduce energy consumption to near zero. A limited set of plant modifications was identified using sensitivity analysis, and the resulting task B system redesign cost significantly less than a full system redesign, while maintaining near-zero energy consumption. The trajectories used here were quintic, placing limitations on dynamic performance. Exploring true upper bounds for control design optimization and co-design performance could be explored using unstructured open-loop control design methods such as direct transcription [2,46].

There are several opportunities for expanding our knowledge regarding the PLCD design methodology. PLCD concepts may apply to a variety of domains beyond mechatronics, and may help inform initial system design to improve the ability to adapt to unanticipated needs [49]. More sophisticated approaches to candidate plant modification selection should be explored, as well as more detailed cost models (both for $C(\mathbf{p})$ used in sensitivity calculation and $\phi(\mathbf{x})$ for PLCD cost minimization). Improved plant design and cost models are under development. More realistic cost models may introduce discontinuities into the cost function. For example, zero plant design change results in zero cost, whereas, any finite change, no matter how small, will result in finite modification cost (i.e., cost jumps from zero to a nonzero value). So far only continuous, high-level plant design changes have been considered. More detailed plant changes present interesting modeling issues. Topological changes, such as adding or removing components, introduce new challenges for co-design solution techniques.

6 Conclusion

In summary, initial PLCD investigations are promising. This methodology has been applied successfully to multiple nonlinear mechatronic systems, and has demonstrated its utility for identifying minimal-cost plant modifications while meeting demanding system requirements. While PLCD has been applied only to mechatronic systems so far, it could be expanded into a more general strategy for strategic redesign of a broader variety of system types, increasing the scope of its applicability and importance.

References

[1] Roos, F., 2007, "Towards a Methodology for Integrated Design of Mechatronic Servo Systems," Ph.D. dissertation, Royal Institute of Technology, Stockholm, Sweden.
[2] Allison, J. T., and Herber, D. R., 2013, "Multidisciplinary Design Optimization of Dynamic Engineering Systems," AIAA J., (to be published).
[3] Li, Q., Zhang, W. J., and Chen, L., 2001, "Design for Control—A Concurrent Engineering Approach for Mechatronic Systems Design," IEEE/ASME Trans. Mechatron., **6**(2), pp. 161–169.
[4] Friedland, B., 1996, *Advanced Control System Design*, Prentice-Hall, Englewood Cliffs, NJ.
[5] Fathy, H. K., Reyer, J. A., Papalambros, P. Y., and Ulsoy, A. G., 2001, "On the Coupling Between the Plant and Controller Optimization Problems," Proceedings of the 2001 American Control Conference, IEEE.
[6] Fathy, H. K., 2003, "Combined Plant and Control Optimization: Theory, Strategies and Applications," Ph.D. dissertation, University of Michigan, Ann Arbor, MI.
[7] Peters, D. L., Papalambros, P. Y., and Ulsoy, A. G., 2009, "On Measures of Coupling Between the Artifact and Controller Optimal Design Problems," Proceedings of the 2009 ASME Design Engineering Technical Conference.
[8] Reyer, J. A., Fathy, H. K., Papalambros, P. Y., and Ulsoy, A. G., 2001, "Comparison of Combined Embodiment Design and Control Optimization Strategies Using Optimality Conditions," Proceedings of the 2001 ASME Design Engineering Technical Conferences.
[9] Peters, D. L., Papalambros, P. Y., and Ulsoy, A. G., 2011, "Control Proxy Functions for Sequential Design and Control Optimization," ASME J. Mech. Des., **133**(9), p. 091007.
[10] Allison, J. T., 2013, "Engineering System Co-Design With Limited Plant Redesign," Eng. Optimiz., ePub.
[11] Li, Y., and Bone, G. M., 2001, "Are Parallel Manipulators More Energy Efficient?," Proceedings of the 2001 IEEE International Symposium on Computational Intelligence in Robotics and Automation.
[12] Spong, M. W., Hutchinson, S., and Vidyasagar, M., 2005, *Robot Modeling and Control*, John Wiley & Sons, New York.
[13] Field, G., and Stepanenko, Y., 1996, "Iterative Dynamic Programming: An Approach to Minimum Energy Trajectory Planning for Robotic Manipulators," Proceedings of the 1996 IEEE International Conference on Robotics and Automation.
[14] Ahmadi, M., and Buehler, M., 1999, "The ARL Monopod II Running Robot: Control and Energetics," Proceedings of 1999 IEEE International Conference on Robotics and Automation.
[15] Barili, A., Ceresa, M., and Parisi, C., 1995, "Energy-Saving Motion Control for an Autonomous Mobile Robot," IEEE International Symposium on Industrial Electronics.
[16] Mei, Y., Lu, Y., Hu, Y. C., and Lee, C. S. G., 2004, "Energy-Efficient Motion Planning for Mobile Robots," Proceedings of the 2004 IEEE International Conference on Robotics and Automation.
[17] Mei, Y., Lu, Y., Lee, C. S. G., and Hu, Y. C., 2006, "Energy-Efficient Mobile Robot Exploration," Proceedings of the 2006 IEEE International Conference on Robotics and Automation.
[18] Ooi, C. C., and Schindelhauer, C., 2009, "Minimal Energy Path Planning for Wireless Robots," Mobile Netw. Appl., **14**(3), pp. 309–321.
[19] Grieco, J. C., Prieto, M., Armada, M., and Gonzalez de Santos, P., 1998, "A Six-Legged Climbing Robot for High Payloads," Proceedings of the 1998 IEEE International Conference on Control Applications.
[20] Pitti, A., and Lungarella, M., 2006, "Exploration of Natural Dynamics Through Resonance and Chaos," Proceedings of the 9th Conference on Intelligent Autonomous Systems.
[21] Sarkar, N., and Podder, T. K., 2001, "Coordinated Motion Planning and Control of Autonomous Underwater Vehicle-Manipulator Systems Subject to Drag Optimization," IEEE J. Ocean. Eng., **26**(2), pp. 228–239.
[22] Mattila, J., and Virvalo, T., 2000, "Energy-Efficient Motion Control of a Hydraulic Manipulator," Proceedings of the 2000 IEEE International Conference on Robotics and Automation.
[23] Sato, A., Sato, O., Takahashi, N., and Kono, M., 2007, "Trajectory for Saving Energy of a Direct-Drive Manipulator in Throwing Motion," Artif. Life Rob., **11**, pp. 61–66.
[24] Agrawal, S. K., Gardner, G., and Pledgie, S., 2001, "Design and Fabrication of an Active Gravity Balanced Planar Mechanism Using Auxiliary Parallelograms," ASME J. Mech. Des., **123**(4), pp. 525–528.
[25] Agrawal, S. K., and Fattah, A., 2004, "Gravity-Balancing of Spatial Robotic Manipulators," Mech. Mach. Theory, **39**(12), pp. 1331–1344.
[26] Fattah, A., and Agrawal, S. K., 2006, "Gravity-Balancing of Classes of Industrial Robots," Proceedings 2006 IEEE International Conference on Robotics and Automation.
[27] Tepper, F. R., and Lowen, G. G., 1972, "General Theorems Concerning Full Force Balancing of Planar Linkages by Internal Mass Redistribution," ASME J. Eng. Ind., **94**, pp. 789–796.
[28] Chung, W. K., and Cho, H. S., 1987, "On the Dynamics and Control of Robotic Manipulators with an Automatic Balancing Mechanism," Proc. Inst. Mech. Eng., Part B (Manage. Eng. Manuf.), **201**(12), pp. 25–34.
[29] Lim, T. G., Cho, H. S., and Chung, W. K., 1990, "Payload Capacity of Balanced Robotic Manipulators," Robotica, **8**(2), pp. 117–123.
[30] Coello, C. A., Christiansen, A. D., and Aguirre, A. H., 1998, "Using a New GA-Based Multiobjective Optimization Technique for the Design of Robot Arms," Robotica, **16**(4), pp. 401–414.

[31] Ravichandran, T., Wang, D., and Heppler, G., 2006, "Simultaneous Plant-Controller Design Optimization of a Two-Link Planar Manipulator," Mechatronics, **16**(3-4), pp. 233–242.
[32] van der Wijk, V., and Herder, J. L., 2009, "Synthesis of Dynamically Balanced Mechanisms by Using Counter-Rotary Countermass Balanced Double Pendula," ASME J. Mech. Des., **131**(11), p. 111003.
[33] McGeer, T., 1990, "Passive Dynamic Walking," Int. J. Robot. Res., **9**(2), pp. 62–82.
[34] Collins, S., Ruina, A., Tedrake, R., and Wisse, M., 2005, "Efficient Bipedal Robots Based on Passive-Dynamic Walkers," Science, **307**(5712), pp. 1082–1085.
[35] Smith, M. J., Grigoriadis, K. M., and Skelton, R. E., 1991, "The Optimal Mix of Passive and Active Control in Structures," Proceedings of the 1991 American Control Conference, IEEE, pp. 1459–1464.
[36] Williamson, M. M., 2003, "Oscillators and Crank Turning: Exploiting Natural Dynamics With a Humanoid Robot Arm," Philos. Trans. R. Soc. London, **361**(1811), pp. 2207–2223.
[37] Park, J. H., and Asada, H., 1994, "Concurrent Design Optimization of Mechanical Structure and Control for High Speed Robots," ASME J. Dyn. Syst., Meas., Control, **116**(3), pp. 344–356.
[38] Giffin, M., de Weck, O., Bounova, G., Keller, R., Eckert, C., and Clarkson, P. J., 2009, "Change Propagation Analysis in Complex Technical Systems," ASME J. Mech. Des., **131**(8), p. 081001.
[39] Siddiqi, A., Bounova, G., de Weck, O. L., Keller, R., and Robinson, B., 2011, "A Posteriori Design Change Analysis for Complex Engineering Projects," ASME J. Mech. Des., **133**(10), p. 101005.
[40] Allison, J. T., and Nazari, S., 2010, "Combined Plant and Controller Design Using Decomposition-Based Design Optimization and the Minimum Principle," Proceedings of the 2010 ASME Design Engineering Technical Conference, Paper No. DETC2010-28887.
[41] Antoulas, A. C., 2005, *Approximation of Large-Scale Dynamical Systems*, SIAM, Philadelphia, PA.
[42] Papalambros, P. Y., and Wilde, D., 2000, *Principles of Optimal Design: Modeling and Computation*, 2nd ed., Cambridge University Press, Cambridge, UK.
[43] Philpott, M. L., Warrington, C. S., Branstad, E. A., David, R., and Nita, R. P., 1996, "A Parametric Contract Modeler for DFM Analysis," J. Manuf. Syst., **15**(4), pp. 256–267.
[44] Boothroyd, G., and Dewhurst, P., 2010, *Product Design for Manufacture and Assembly*, 3rd ed., CRC Press, Boca Raton, FL.
[45] Allison, J. T., 2012, "Simulation and Limited Redesign of a Counterbalanced Two Link Robotic Manipulator," http://www.mathworks.com/matlabcentral/fileexchange/37665
[46] Allison, J. T., and Han, Z., 2011, "Co-Design of an Active Suspension Using Simultaneous Dynamic Optimization," Proceedings of the 2011 ASME Design Engineering Technical Conference, Paper No. DETC2011-48521.
[47] Deshmukh, A. P., and Allison, J. T., 2013, "Design of Nonlinear Dynamic Systems using Surrogate Models of Derivative Functions," Proceedings of the 2013 ASME Design Engineering Technical Conference, Paper No. DETC2013-12262.
[48] Arai, H., and Tachi, S., 1991, "Position Control of a Manipulator With Passive Joints Using Dynamic Coupling," IEEE Trans. Rob. Autom., **7**(4), pp. 528–534.
[49] Harper, S. R., and Thurston, D. L., 2008, "Incorporating Environmental Impacts in Strategic Redesign of an Engineered System," ASME J. Mech. Des., **130**(3), p. 031101.